Applied Physics A (2025) 131:51
https://doi.org/10.1007/s00339-024-08179-y

Effect of P_2O_5 addition on anorthite based glass-ceramic glazes

Betül Yıldız[1] · **Zehra Emel Oytaç**[2] · **Zahide Bayer Öztürk**[3]

Received: 29 July 2024 / Accepted: 13 December 2024 / Published online: 23 December 2024

Abstract
Anorthite-based glazes are highly valued in the ceramics industry for their ease of crystallization under fast-firing conditions and their ability to impart excellent mechanical and aesthetic properties. This study investigates the effects of P_2O_5 on the thermal properties, microstructure, microhardness, and optical characteristics of anorthite-based glazes. The results indicate that the addition of P_2O_5 led to a reduction in both the glass transition temperature and crystallization temperature of the glazes. Furthermore, the increased intensity of the exothermic peak associated with crystallization suggests a greater amount of crystal formation in the P_2O_5-added glazes. In all compositions, anorthite was identified as the dominant phase. Moreover, an increased P_2O_5 content resulted in a higher number of anorthite crystals, while concurrently reducing their size. Glazes with P_2O_5 addition exhibited higher hardness values compared to those without P_2O_5. This outcome is attributed to the enhanced crystallization of the anorthite phase, as confirmed by DTA, XRD, and SEM analyses.

Keywords Ceramic tile · Fast firing · Glass-ceramic glaze · Anorthite · Nucleating agents · P_2O_5

1 Introduction

Glazes are durable glassy coatings that enhance both the technical performance and aesthetic appeal of ceramic products. Typically, glazes consist of one or more layers applied to achieve a total thickness ranging from 75 to 500 µm, effectively covering ceramic tiles and providing them with a smooth and protective finish [1]. The raw materials used in glaze formulations include feldspar, calcite, magnesite, quartz, alumina, and various frits [2].

Glass-ceramics are ceramic materials created by controlling crystallization in base glass (nucleation and crystal growth) [1]. Various functionalities discovered in glass-ceramics have enabled their use in diverse applications [3–10]. A significant application of glass-ceramics is the development of high-hardness and abrasion-resistant glass-ceramic glazes to enhance the performance of traditional glazes [1, 11]. The design of a glass-ceramic glaze should ensure technical and commercial compatibility with manufacturing conditions typically used in industrial production, where precursor frits consolidate the glazes through a single heating process [1].

Glazes can be classified based on their optical properties such as gloss, color, or opacity [1]. Ceramic glazes used in industry are generally classified as transparent matte, transparent glossy, opaque matte, and opaque glossy according to their optical characteristics. Transparent glaze is one of the most important types in the ceramic tile sector. It is commonly applied over decorative layers to provide a smooth and easy-to-clean surface while achieving excellent decorative effects. Therefore, the performance of transparent glaze is essential for ceramic tiles. Transparent glaze mainly comprises an amorphous glass phase that exhibits weak mechanical properties and limited chemical stability. This characteristic limits its durability and suitability for high-traffic areas like squares or airports, affecting the tiles' lifespan and application [11]. Consequently, enhancing the characteristics of transparent glaze, particularly its mechanical strength, remains a critical objective for the tile industry.

Transparent glazes are commonly made from frits that do not crystallize during firing and typically have a hardness of up to 6 GPa, showing low abrasion resistance. In contrast, glazes containing frits that fully or partially crystallize during firing generally exhibit much improved mechanical

✉ Betül Yıldız
betul.yildiz@bilecik.edu.tr

[1] Metallurgy and Materials Engineering Department, Bilecik Şeyh Edebali University, Bilecik, Türkiye

[2] NG Kütahya Seramik Inc. R&D Center, Kütahya, Türkiye

[3] Nevsehir Hacı Bektas Veli University, Nevsehir, Türkiye

Table 1 Initial frit chemical composition (S)

	SiO_2	Al_2O_3	CaO	MgO	Na_2O	K_2O	ZnO
wt%	45–55	15–20	15–20	0–5	0–5	0–5	5–10

properties. This is because they form a composite structure with crystalline phases or an amorphous phase surrounded by crystalline phases [12].

The tendency and rate of crystallization largely depend on the chemical composition of the frit. The closer the composition of the glass to crystalline silicate minerals, the faster the crystalline phase develops. Therefore, in glass-ceramic glazes, the most common crystalline phases include zircon ($ZrSiO_4$), anorthite ($CaAl_2Si_2O_8$), wollastonite ($CaSiO_3$), celsian ($BaAl_2Si_2O_8$), leucite ($KAlSi_2O_6$), cordierite ($Mg_2Al_4Si_5O_{18}$), and mullite ($Al_6Si_2O_{13}$) [1].

Anorthite ($CaO{\cdot}Al_2O_3{\cdot}2SiO_2$), with a Mohs hardness of 6, a thermal expansion coefficient of 4.5×10^{-6}/°C, and a refractive index of 1.57, close to 1.51 for glass phase, is a frequently occurring crystal in ceramic materials. Anorthite-type glass-ceramics are characterized by high mechanical strength and good chemical resistance [1], making them suitable choices for developing transparent glass-ceramic glazes with high hardness for ceramic tiles [11].

Anorthite-based glazes have been extensively studied in the literature due to their ease of crystallization of the anorthite phase in ceramic glazes under industrial rapid firing kiln regimes, and their ability to impart good mechanical and aesthetic properties to the glaze structure [11–17]. The crystallization characteristic is significantly influenced by the composition of the base glass, including nucleating agents and glass network formers [18].

A nucleating agent is a component within a glass composition that serves to enhance internal nucleation rates or precipitation. It facilitates the controlled formation of desired crystal phases by reducing the thermodynamic or kinetic barriers to nucleation, often through a combination of mechanisms [19]. A literature review indicates a wide range of chemicals such as TiO_2, CaF_2, ZrO_2, P_2O_5, Cr_2O_3, Fe_2O_3, V_2O_5, and MoO_3 can serve as nucleating agents [20].

In the literature, the effects of various nucleating agents have been studied in anorthite-based glass, glass-ceramic, and glass-ceramic glazes [18, 20–28]. According to our research, when examining glazes with nucleating agent additions, specifically in anorthite-based glazes, it was observed that Kim et al. examined the effect of TiO_2 [25], Bao et al. investigated the effect of ZnO [26], and Silakate et al. explored the effect of Fe_2O_3 [28].

P_2O_5 is commonly used as a nucleating agent in the preparation of transparent glass-ceramics. It typically induces phase separation during nucleation, promoting crystallization of the glasses. Additionally, P_2O_5 does not impart color to glasses or glass-ceramics [29]. The aim of this work is to understand the role of P_2O_5 addition on the thermal behavior, microstructure, aesthetic properties, and microhardness of anorthite-based glass-ceramic glazes. To achieve this aim, anorthite based glass ceramic glazes with different compositions were fabricated from the frit and industrial raw materials. These glazes were subjected to sintering under an industrial rapid-firing porcelain tile regime. Detailed investigations were conducted to analyze the microstructural and optical properties of the resultant glazes.

Table 2 Nucleating agent added per 100 g of glass batch (wt%)

Raw materials/codes	S	*P*-1	*P*-2	*P*-3
P_2O_5	-	3	6	9

Table 3 The weight-based material ratios used in glaze preparation

Material	wt%
Frit	92
Kaolin (for glaze)	8
Carboxyl methyl cellulose	0.1
Sodium tripolyphosphate	0.2

2 Materials and methods

2.1 Frit and glaze preparation

The raw materials used in frit and glaze production; quartz, alumina, calcite, sodium carbonate and zinc oxide were supplied from a Ceramic Factory (NG Kutahya, Turkey). The P_2O_5 used in the study was obtained from Sigma-Aldrich (Assay ≥ 97.0% (acidimetric)). Frit batches were prepared according to the desired oxide percentages based on the chemical analysis results of the raw materials. Frit batches were weighed in 250 g.; after mixing for homogenization, they were placed into ceramic crucibles. The obtained batches were melted in a glass melting furnace at 1450 °C (Protherm PLF 160/9 was melted) and held at peak temperature for one hour, then quenched in water to form frit. The effect P_2O_5 nucleating addition in the standard frit recipe (S) was investigated in this study. Frit recipes containing wt% 0, 3, 6 and 9 P_2O_5 were respectively labeled as S, P1, P2, and P3. The chemical composition range of the initial frit and weight percents of frits' nucleating agents were presented in Tables 1 and 2, respectively.

The frits were loaded into alumina ball mills in the proportions given in Table 3 and subjected to grinding for 15 min to obtain glaze slurries. Glaze recipes prepared with S, P-1, P-2 and P-3 frits were respectively labeled as GS, GP-1, GP-2, and GP-3. The solid-to-water ratio of the

prepared glazes was kept at approximately 70%. The density of the glazes was adjusted to approximately 1800 g/l. The prepared glazes were applied to engobed porcelain tiles using a ragle with a 0.6 cm opening, and subjected to a total of 40 min firing at a peak temperature of 1195 °C in the porcelain tile firing regime at the ceramic factory (NG Kutahya Factory).

2.2 Thermal characterization

The thermal properties of the samples were analyzed using a heating microscope (Misura 3 HSM Hot-stage microscopy, Expert Systems, Srl, Modena, Italy) and a differential thermal analysis (DTA) (STA 409 PG Netzsch). Glaze powders were prepared by uniaxial dry pressing into cylindrical molds (2 mm x 3 mm) and then heated in the microscope, with temperature increasing from room temperature to 1300 °C at a rate of 10 °C per minute. Automatic software analysis (Misura 3.32) was used to determine the characteristic temperatures of the samples based on their geometric parameters.

DTA analysis was performed up to 1300 °C with a heating rate of 10 °C/min under constant airflow. The glass transition temperature (Tg) and crystallization peak temperature (Tc) of the frit samples were determined in the temperature range of 40–1300 °C using DTA, employing a heating rate of 10 °C/min under a constant flow of nitrogen gas. Approximately 15 mg of frit powders, sieved through a 120 mesh sieve, were loaded into an alumina crucible for DTA testing under an air atmosphere, with high purity Al_2O_3 serving as the reference material.

2.3 Characterization of fired glazed samples

The color parameters L*, a*, and b* and the glossiness of the samples (measured at a 60° angle) were determined using a Konica Minolta Spectro Photometer CM 600D model color measurement device.

The mineralogical phase analyses of fired glazes were carried out between 10° and 90° at a scanning speed of 2°/min using the Rigaku Miniflex 600 diffractometer at 40 kV and 15 mA. For microstructural analysis, all samples were sectioned from glazed tiles and polished from the cross-section surface. All samples were subjected to coating with gold/palladium (Au/Pd) or carbon (C) using the LEICA EM ACE600 & POLARON SC7620 coating device to ensure surface conductivity. Microstructure analyses of the samples were performed using a scanning electron microscope (ZEISS, SUPRA 50 VP), and the backscattered electron image (BSE mode) method, which separates phases based on atomic weight, was used for analysis. The microhardness of the glazes was measured using an micro-Vickers hardness tester (EMCOTEST DuroScan 20) with a dwell time of 3 s. Three measurements were taken to determine the microhardness of the glazes, and their averages have been included in the study.

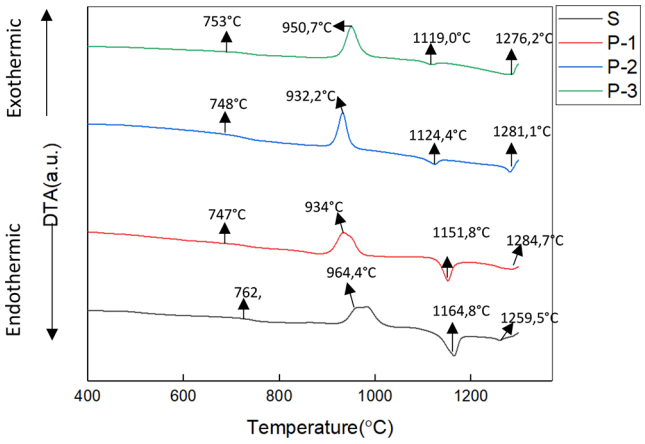

Fig. 1 DTA curves of powdered frits

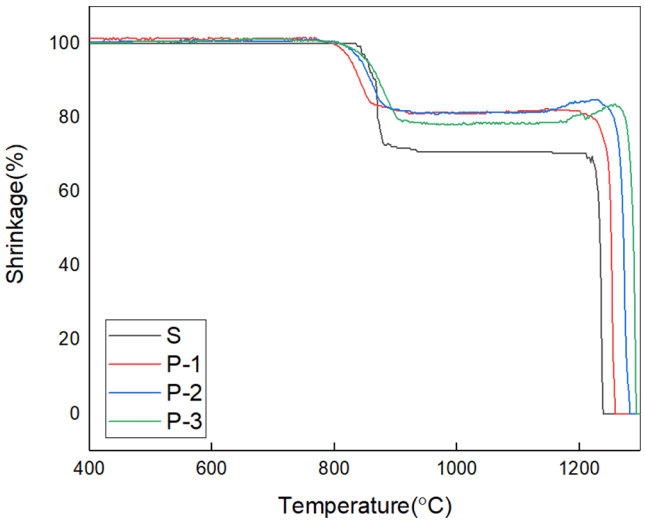

Fig. 2 Hot-stage microscopy shrinkage curves of powdered frits

3 Results and discussions

3.1 Role of P2O5 on thermal behaviour of frits

In the study, differential thermal analysis (DTA) and hot-stage microscopy (HSM) were used to examine the thermal behaviors of the frits. The DTA analysis determined, in sequence, the glass transition temperature, crystallization temperature, crystal melting temperature, and fusion temperature of the frits. Using HSM, the sintering, softening, and melting temperatures were found, respectively. The influence of the P_2O_5 content on the thermal behavior of the analyzed glazes is illustrated in Figs. 1 and 2; Table 4.

Table 4 Characteristic temperatures of powdered frits derived from DTA and HSM (°C)

	$T_{Glass\ Transition}$	$T_{Sintering}$	$T_{Softening}$	$T_{Crystallization}$	$T_{Crystal\ Melting}$	$T_{Melting}$	T_{Fusion}
S	762	857	859	964.4	1164.8	1290	1259.5
P-1	747	829	835	934.0	1151.8	1253	1284.7
P-2	748	847	851	932.2	1124.4	1275	1281.1
P-3	753	857	861	950.7	1190.0	1290	1276.2

The DTA curves of frits S, P-1, P-2, and P-3 with a heating rate of 10 °C/min are shown in Fig. 1. In glazes, densification occurs through sintering facilitated by viscous flow at temperatures just above the glass transition temperature (T_g), resulting in a densely packed layer with minimal porosity [1]. Glass transition temperatures of the glazes for S, P-1, P-2 and P-3 were detected as 762, 747, 748 and 753 °C respectively. The initial exothermic peak observed in the samples indicates the onset of crystallization, with the first crystallization temperatures for samples S, P-1, P-2, P-3, and P-4 recorded as 964.4, 934, 932.2 and 950.7 °C respectively (Fig. 1). It has been determined that samples containing P_2O_5 exhibit lower glass transition temperature and crystallization temperature compared to the initial frit. However, an increase in the amount of P_2O_5 did not show a linear change in glass transition temperature and crystallization temperature. In the study, the crystalline melting temperatures of the glazes were found to range between 1119 and 1165 °C, while the glaze melting temperatures ranged between 1259 and 1285 °C. An increase in the amount of P_2O_5 in glaze compositions has shown a decrease in crystalline melting temperatures and an increase in glaze melting temperatures (Fig. 1).

The hot stage microscope is essential in this process, offering critical insights into the sintering of grains (starting from milled material), the softening of the glaze sample, and the specific temperatures or intervals at which these events take place [30]. Hot stage microscopy curves are depicted in Fig. 2. Standard frit without P_2O_5 addition (S frit) exhibits higher shrinkage compared to all samples. This phenomenon is attributed to crystallization. Samples with nucleating agents crystallized earlier, as depicted in Fig. 1, and once crystallization initiates, sintering is impeded [31]. The sintering and softening temperatures of the glazes studied were determined to be between 829 and 857 °C and 835–861 °C, respectively. Glazes with additions of 3% and 6% P_2O_5 exhibited lower firing and softening temperatures compared to the initial frit, while the temperatures of the glaze with 9% P_2O_5 addition were similar to those of the initial frit (Table 4).

The effect of P_2O_5 on the thermal properties of various glass and glass-ceramic systems has been investigated in many different systems. When evaluating studies on the effect of P_2O_5 on glass-ceramic systems in the literature, it is observed that the variation in temperatures depends on the type and quantity of components in the system, as well as the amount of P_2O_5 used. Some of the studies indicated that crystallization temperature was increased with P_2O_5 content. For instance, Zheng et al. investigated how P_2O_5 affects the Y_2O_3-Al_2O_3-SiO_2 glass-ceramic system. They found that the crystallization peaks gradually shifted to higher temperatures. Analysis using FESEM and XRD showed that higher P_2O_5 content reduced nucleation sites and crystallinity [29]. Thieme et al. [32] included up to 4 mol% P_2O_5 into a BaO-SrO-ZnO-SiO_2 system. They contended that P_2O_5 did not act as a nucleating agent in this system. Thermal analysis showed minimal impact on T_g with increasing P_2O_5 content, but an elevation in T_c and a decrease in the sharpness of exothermic peaks were noted [32]. Specific melting points were not provided in the findings.

On the other hand in some studies, similar to the present investigation, it has been found that the addition of P_2O_5 lowers the crystallization temperature. For instance, Luo et al. studied P_2O_5's effect on Li_2O-SiO_2-Si_3N_4 glass-ceramics, showing it enhances crystallization by lowering activation energy [33]. Bao et al. explored P_2O_5's impact on Li_2O-MgO-Al_2O_3-SiO_2 glass-ceramics, noting a decrease in T_c and melting point with 5 wt% P_2O_5, while the exothermic peak sharpened [34]. Von Clausbruch et al. found 1 mol% P_2O_5 necessary for lath-like lithium disilicate microstructures, observing heterogeneous nucleation with reduced T_c and peak sharpness [35]. Holand et al. studied nucleation in lithium metasilicate and disilicate, reporting increased T_g and reduced T_c with higher P_2O_5 content, with more pronounced exothermic peaks [36]. Fernandes et al. analyzed P_2O_5's effect on these glass-ceramics, noting T_c decrease and sharper exothermic peaks with 1–3 mol% P_2O_5, but unclear effects on T_g and T_m [37]. Ghaebi Panah et al. investigated nucleation using P_2O_5 in photosensitive silicate systems, showing reduced T_c and exothermic peak sharpness without affecting T_g, T_m decreased [38]. Glatz et al. discussed P_2O_5 in Li_2O-Al_2O_3-SiO_2 (LAS) systems, noting varied T_g with minor fluctuations, decreased crystallization temperature under 10 mol% Al_2O_3, and sharper exothermic peaks with more P_2O_5 [39]. Gaddam et al. studied P_2O_5's combined effect with SiO_2-Li_2O ratios on lithium disilicate crystallization, showing shifts in T_g and T_c, sharper exothermic peaks with 1 mol% P_2O_5 [40]. Rampf et al. explored P_2O_5's role in high SiO_2 to Li_2O ratio silicate systems, noting complex trends in T_g and exothermic peak intensity,

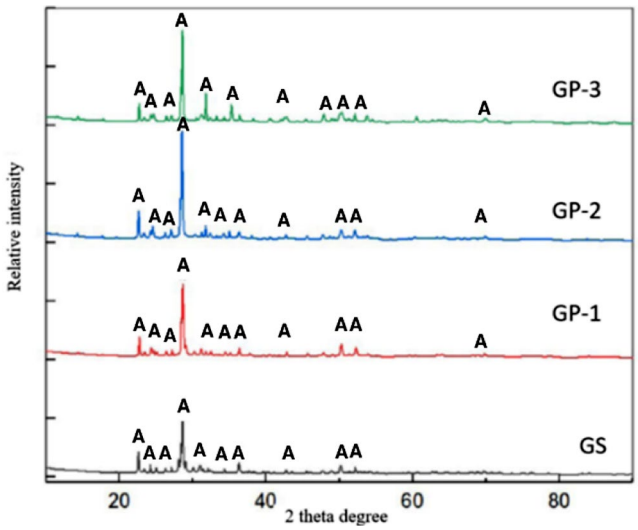

Fig. 3 The XRD analysis results for the glazes containing P_2O_5, (**A**) Anorthite

with melting point decrease as P_2O_5 increased [41]. Zheng et al. examined P_2O_5's impact on lithium disilicate glass-ceramics, observing enhanced nucleation, sharper exothermic peaks, and variable Tc and melting point trends with increasing P_2O_5 content [42].

3.2 Role of P2O5 on microstructure evolution

The XRD analysis results of glazes containing P_2O_5 are given in Fig. 3. The main phase identified in the glazes has been determined as Anorthite (PDF#41-1486). With the inclusion of P_2O_5, ongoing crystallization of anorthite has been observed in the microstructure. As the addition of P_2O_5, the relative peak intensity of anorthite crystals has increased significantly compared to the standard glaze. The glaze containing 6% P_2O_5 exhibited the highest relative peak intensity for the anorthite phase.

The backscattered electron images taken from the cross-sections of glazes containing P_2O_5 are shown in Figs. 4 and 5. When examining the SEM microstructures, it is observed that the pore structures in the glazes do not differ significantly. However, the P-3 glaze exhibits slightly lower porosity (Fig. 4). The light-colored areas in the structure represent the glassy phase, while needle-like crystals depict anorthite crystals. Subsequently, in glazes labeled P-2 and P-3, which contain 6% and 9% P_2O_5 respectively, an enhancement in crystal density is noted alongside a reduction in crystal length (Fig. 5).

Figure 6; Table 5 present the EDS patterns and corresponding oxide weight percentages (wt%) measured in the glaze matrix, while Fig. 7; Table 6 provide the EDS patterns and oxide wt% obtained from the crystalline phases. The detected oxides in both the glassy and crystalline phases include Na_2O, Al_2O_3, SiO_2, CaO, ZnO, and P_2O_5. Notably, the crystalline phases exhibit a higher concentration of Al_2O_3 and a lower concentration of ZnO compared to the glassy matrix.

In the literature exploring the influence of P_2O_5 on microstructure in glass ceramic systems, it is evident that

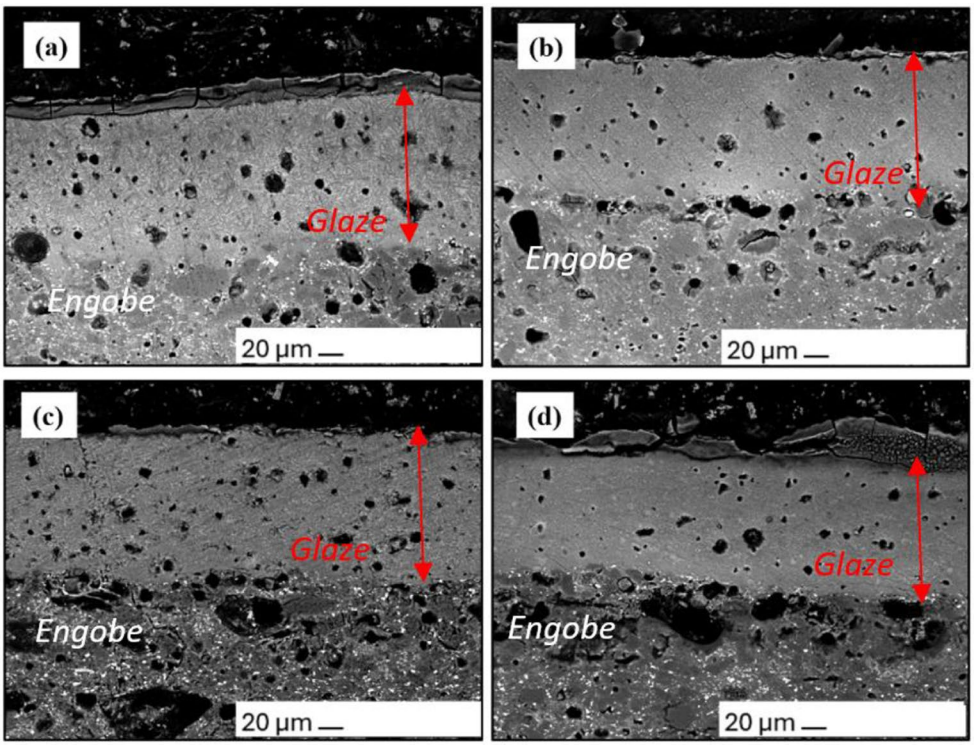

Fig. 4 The backscattered electron images taken from the cross-sections of glazes containing P_2O_5 at a magnification of 1000, (**a**) GS, (**b**) GP-1, (**c**) GP-2, (**d**) GP-3

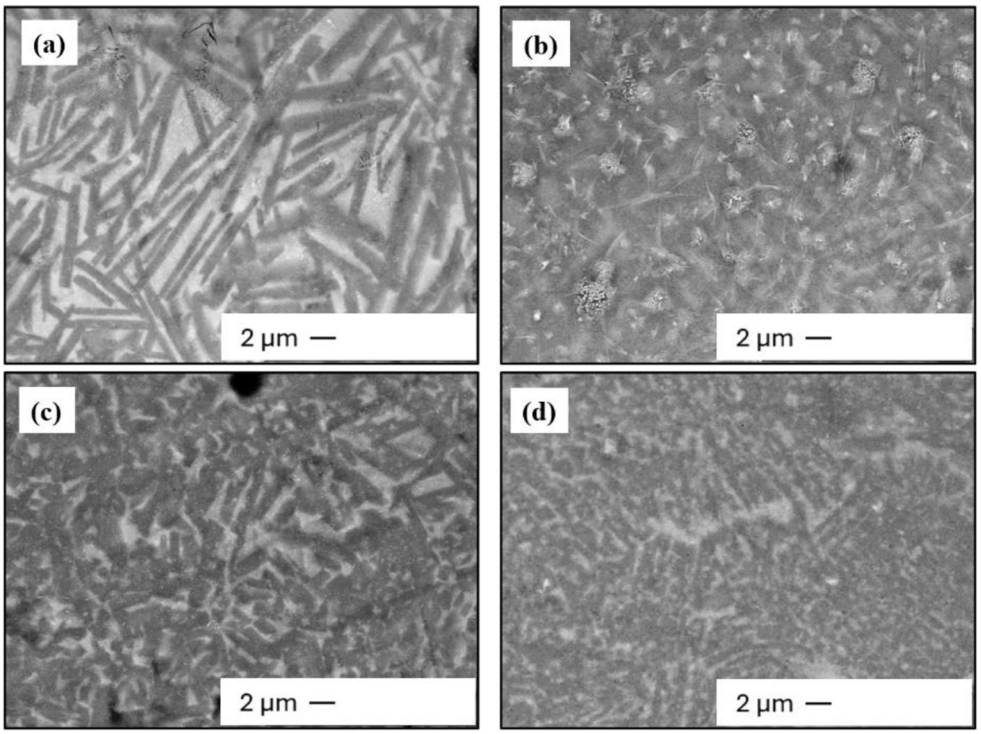

Fig. 5 The backscattered electron images taken from the cross-sections of glazes containing P_2O_5 at a magnification of 10.000, (**a**) GS, (**b**) GP-1, (**c**) GP-2, (**d**) GP-3

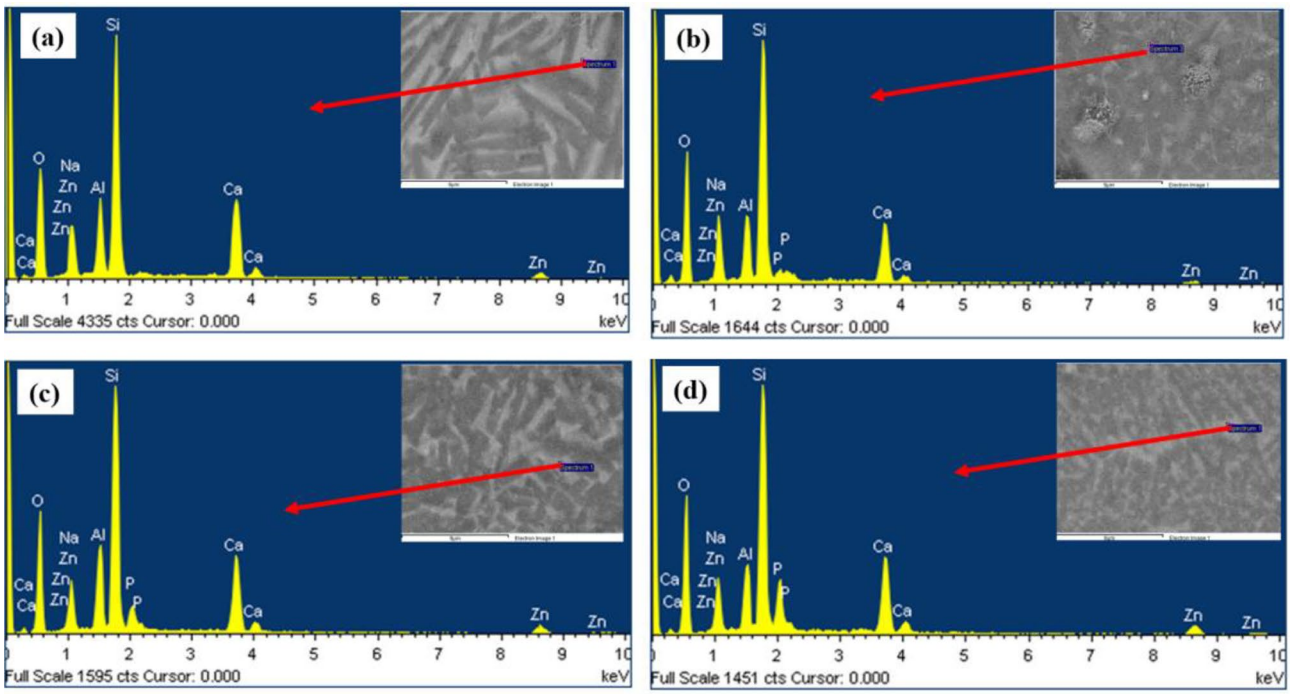

Fig. 6 EDX patterns taken from the EDX patterns of the glazes inhibiting gray regions (glassy phases) (**a**) GS, (**b**) GP-1, (**c**) GP-3, (**d**) GP-4

the microstructure varies significantly based on the system's components, the quantity of P_2O_5 employed, and the firing protocols utilized. Zhang et al. observed that higher levels of P_2O_5 elevated the formation temperature of $LiAlSi_2O_6$ and acted as nucleation sites for Li_2SiO_3 through the formation of Li_3PO_4. This process facilitated the transition from Li_2SiO_3 to $Li_2Si_2O_5$. Concurrently, the phase morphology shifted from lamellar to columnar, eventually forming an interlocking structure during specific heat treatments. These phase transformations and the creation of Li_3PO_4 enhanced cell proliferation, differentiation, and mineralization in glass ceramics. Notably, LS_4 containing 4.12 mol% P_2O_5

Table 5 Weight% of oxides measured in the cross-section of the glassy phase using FESEM-EDX: (a) GS, (b) GP-1, (c) GP-3, (d) GP-4

Oxide%	GS	GP-1	GP-2	GP-3
Na_2O	6.81	12.02	5.91	6.5
Al_2O_3	14.03	12.30	14	10.50
SiO_2	54.25	55.64	49.65	44.90
CaO	17.50	14.25	15.27	14.62
ZnO	7.41	3.35	8.23	10.19
P_2O_5	-	2.45	6.95	13.29

Table 6 Weight% of oxides measured in the cross-section of the crystalline phase using FESEM-EDX: (a) GS, (b) GP-1, (c) GP-3, (d) GP-4

Oxide%	GS	GP-1	GP-2	GP-3
Na_2O	5.37	10.19	7.16	7.12
Al_2O_3	20.91	15.19	19.99	16.76
SiO_2	55.44	56.31	53.03	52.29
CaO	14.71	13.23	13.06	13.35
ZnO	3.57	3.36	3.71	3.76
P_2O_5	-	1.72	3.06	6.72

exhibited a bone-like structure during mineralization, indicating potential orthopedic applications [43].

In another study, Zhang et al. examined the impact of P_2O_5 on the crystallization, structure, and mechanical properties of Yttrium Aluminosilicate (YAS) glasses. FESEM and XRD analyses showed that increased P_2O_5 concentrations decreased nucleation sites and led to reduced crystallinity [29]. In contrast, Luo et al. investigated the crystallization kinetics and behavior of P_2O_5-added Li_2O-SiO_2-Si_3N_4 glass. Their research revealed that incorporating P_2O_5 as a nucleating agent enhanced crystallization ability and reduced the activation energy required for crystallization. As the P_2O_5 content increased (from 0 to 3.0 mol%), the crystallization temperature decreased due to heterogeneous nucleation facilitated by Li_3PO_4 crystals. Higher concentrations of P_2O_5 promoted increased nucleation but slowed the kinetics of crystal growth, leading to a microstructural transition from plate-like crystal aggregates to interlocking rod-like crystals [33].

3.3 Role of P2O5 on color measurements

The color parameter values and surface properties are detailed in Table 5. In the CIELAB model, L* = 0 corresponds to black, L* = 100 corresponds to white, a* represents the green-red axis horizontally, and b* represents the yellow-blue axis vertically [44]. Generally, it is observed that, the opacity properties of the glazes are low (with low L* values). For assessing the transparency levels of the glazes, we computed ΔE data based on the L*, a*, b* color values of both the engobe surface and the glaze surface. As the amount of ΔE increases, the opacity of the glaze increases. All the glazes in the study exhibited a transparent and matte character. All the glazes used in the study showed a gloss value for 60° below 5 (Table 7).

3.4 Role of P2O5 on microhardness of glazes

The microhardness of the glazes is presented in Table 8. It is well established that the hardness of glass-ceramic glazes

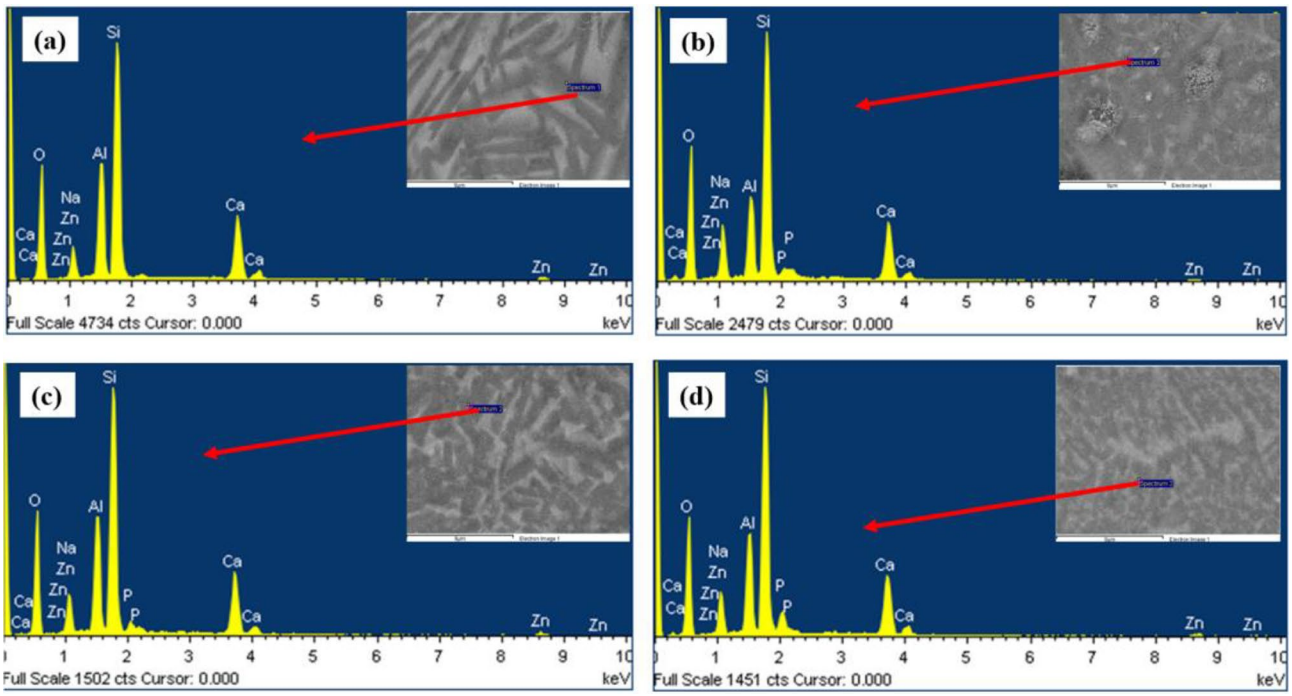

Fig. 7 EDX patterns taken from the EDX patterns of the glazes inhibiting dark regions (crystalline phases) (**a**) GS, (**b**) GP-1, (**c**) GP-3, (**d**) GP-4

Table 7 Color values and surface properties of glazes with nucleating agent additions after firing

Surface	Colour coordinates				
	L	a*	b*	ΔE	Gloss (60°)
Engobe	83.02	0.18	3.34	-	-
GS	82.87	-0.26	1.86	1.55	3.5
GP-1	84.39	-0.34	1.93	2.03	3.9
GP-2	85.33	-0.34	1.91	2.77	3.2
GP-3	84.90	-0.37	1.97	2.39	3.7

Table 8 Vickers hardness of glazes

Surface	Microhardness (HV)
GS	721.00
GP-1	785.33
GP-2	744.60
GP-3	751.00

is influenced by both the type and content of the crystalline phases present. In this study, hardness values ranged from 721 to 785.33 HV. Notably, glazes with P_2O_5 addition exhibited higher hardness values than those without P_2O_5. This result can be attributed to the increased crystallization of the anorthite phase, as confirmed by XRD and SEM analyses. The microhardness values obtained are consistent with the findings reported in the literature.

Wang et al. investigated the microhardness of transparent glass-ceramic glazes based on anorthite. They observed that using of high-calcium frit promotes the crystallization of anorthite, thereby improving the glaze's hardness. Their findings revealed that increased crystallization of anorthite enhances the hardness of the glaze, with reported values ranging from 6.4 to 8.1 GPa [11]. Similarly, Gajek et al. examined the microhardness of anorthite-based glazes, reporting values between 6.57 and 8.01 GPa [12]. Son and Kim also explored the crystallization and hardness of CaO-Al_2O_3-SiO_2-ZnO-based glasses in relation to the substitution of the nucleating agent TiO_2. Their study showed a marked increase in overall crystallinity, from 57.9 to 83.8%, accompanied by a significant rise in hardness, from 3.12 GPa to 6.89 GPa, as a result of TiO_2 substitution [25].

Additionally, Bao et al. found that the Vickers hardness of glazes improved significantly, from 5.26 GPa to 7.20 GPa, due to the crystallization of anorthite, attributing the enhancement to the crystallization of anorthite rather than diopside [26]. Furthermore, Wang et al. reported an increase in Vickers hardness from 662.8 to 683 HV in anorthite-based glass ceramics when compared to Cr_2O_3-free glass ceramics [24].

4 Conclusions

The properties of glass-ceramic glazes are significantly influenced by the presence of nucleating agents. The addition of such agents promotes the development of fine-grained structures within these materials. The findings of this study demonstrate that glazes containing P_2O_5 exhibit lower glass transition and crystallization temperatures compared to the original glaze composition. This suggests that P_2O_5 facilitates the formation of crystal phases at lower temperatures and enhances crystallization tendencies. XRD analysis confirms that increasing P_2O_5 content accelerates the crystallization of anorthite phase. Moreover, SEM analysis revealed that higher P_2O_5 concentrations contribute to a denser crystalline microstructure. These observations suggest that P_2O_5 plays a pivotal role in promoting anorthite formation. Glazes incorporating P_2O_5 also exhibited higher microhardness values compared to those without it. Importantly, this improvement in microhardness was achieved without compromising the transparency of the glazes. The insights gained from this study offer valuable implications for both ceramic tile manufacturers and researchers in the field of glass-ceramic materials.

Author contributions All authors contributed to the study conception and design. Material preparation, data collection, resources and analysis were performed by B. Yıldız and Z.E. Oytaç. Z.B. Öztürk, B. Yıldız and Z.E. Oytaç contributed in conceptualization, investigation, methodology, data curation, writing—original draft, writing—review, editing, validation.

Funding This research was supported by the Scientific Research Projects Coordination Unit (BAP) of Bilecik Şeyh Edebali University under grant number 2023-01.BŞEÜ.03–11.

Data availability Not applicable.

Declarations

Competing interest The authors declare that they have no known competing financial interests or personal relationships that could have appeared to influence the work reported in this paper.

References

1. R. Casasola, J. Ma Rincon, M. Romero, Glass–ceramic glazes for ceramic tiles: a review. J. Mater. Sci. **47**, 553–582 (2012). https://doi.org/10.1007/s10853-011-5981-y
2. B. Yazırlı, H. Sarı, K. Kayacı, F. Kara, Effect of nucleating agent additions on gahnite based glass-ceramic glazes. J. Eur. Ceram. Soc. **44**, 3344–3351 (2024)
3. V. Fuertes, M.J. Cabrera, J. Seores, D. Munoz, J.F. Fernandez, E. Enriquez, Enhanced wear resistance of engineered glass-ceramic by nanostructured self-lubrication. Mater. Des. **168**, 107623 (2019)

4. H. Bach, D. Krause, Low Therm. Expansion Glass Ceram. (2005). https://doi.org/10.1007/3-540-28245-9
5. W. Höland, G. Beall, Glass–Ceramic Technology, 2012
6. R. Lisiecki, E. Czerska, M. Żelechower, R. Swadźba, W. Ryba-Romanowski, Oxyfluoride silicate glasses and glass-ceramics doped with erbium and ytterbium - an examination of luminescence properties and up-conversion phenomena. Mater. Des. **126**, 174–182 (2017). https://doi.org/10.1016/j.matdes.2017.04.046
7. O. Bretcanu, S. Spriano, C.B. Vitale, E. Verné, Synthesis and characterization of coprecipitation-derived ferrimagnetic glass-ceramic. J. Mater. Sci. **41**, 1029–1037 (2006). https://doi.org/10.1007/s10853-005-2636-x
8. R.D. Rawlings, J.P. Wu, A.R. Boccaccini, Glass-ceramics: their production from wastes-a review. J. Mater. Sci. **41**, 733–761 (2006). https://doi.org/10.1007/s10853-006-6554-3
9. V. Fuertes, M.J. Cabrera, J. Seores, D. Muñoz, J.F. Fernández, E. Enríquez, Hierarchical micro-nanostructured albite-based glass-ceramic for high dielectric strength insula_tors. J. Eur. Ceram. Soc. **38**, 2759–2766 (2018). https://doi.org/10.1016/j.jeurceramsoc.2018.02.009
10. I. Rozenstrauha, L. Krage, E. Lodins, V. Filipenkov, Functional properties of glassceramics for building application, Proc. 2nd Int. Conf. Adv. Constr. 2010, pp. 141–147
11. S. Wang, X. Li, C. Wang, M. Bai, X. Zhou, X. Zhang, Y. Wang, Anorthite based transparent glass-ceramic glaze for ceramic tiles: Preparation and crystallization mechanism. J. Eur. Ceram. Soc. **42**, 1132–1140 (2022)
12. M. Gajek, A. Rapacz-Kmita, E. Stodolak-Zych, M. Zarzecka-Napierała, M. Wilk, A. Magdziarz, M. Dudek, Microstructure and mechanical properties of diopside and anorthite glazes with high abrasion resistance. Ceram. Int. **48**, 6792–6798 (2022)
13. L. Fröberg, L. Hupa, M. Hupa, Corrosion of the crystalline phases of matte glazes in aqueous solutions. J. Eur. Ceram. Soc. **29**, 7–14 (2009). https://doi.org/10.1016/j.jeurceramsoc.2008.04.037
14. J. Reinosa, F. Rubio-Marcos, E. Solera, M.A. Bengochea, J.F. Fernandez, Sintering behaviour of nanostructured glass-ceramic glazes. Ceram. Int. **36**, 1845–1850 (2010)
15. M. Gajek, J. Partyka, A. Rapacz-Kmita, K. Gasek, Development of anorthite based white porcelain glaze without $ZrSiO_4$ content. Ceram. Int. **43**, 1703–1709 (2017)
16. M.G. Rasteiro, T. Gassman, R. Santos, E. Antunes, Crystallization phase characterization of glass-ceramic glazes. Ceram. Int. **33**, 345–354 (2007). https://doi.org/10.1016/j.ceramint.2005.10.002
17. A. Tunali, E. Ozel, Production and characterisation of granulated frit to achieve anorthite based glass–ceramic glaze. J. Eur. Ceram. Soc. **35**, 1089–1095 (2015)
18. C. Lo, J. Duh, B. Chiou, W. Lee, Microstructure characteristics for anorthite composite glass with nucleating agents of TiO_2 under non-isothermal crystallization. Mater. Res. Bull. **37**, 1949–1960 (2002)
19. A.V. DeCeanne, R. Lorena, J. Rodrigues, Collin, J.C. Wilkinson, E.D. Mauro, Zanotto, Examining the role of nucleating agents within glass-ceramic systems. J. Non-cryst. Solids. **591**, 121714 (2022)
20. D.P. Mukherjee, S.K. Das, SiO_2–Al_2O_3–CaO glass-ceramics: Effects of CaF_2 on crystallization, microstructure and properties. Ceram. Int. **39**, 571–578 (2013)
21. Y. Luo, F. Wang, Q. Liao, L. Liu, Y. Wang, J. Zhou, Y. Xu, H. Zhu, Y. Gu, Effect of TiO_2 on crystallization kinetics, microstructure and properties of building glass-ceramics based on granite tailings. J. Non-cryst. Solids. **572**, 121092 (2021)
22. G.A. Khater, Influence of Cr_2O_3, LiF, CaF_2 and TiO_2 nucleants on the crystallization behavior and microstructure of glass-ceramics based on blast-furnace slag. Ceram. Int. **37**, 2193–2199 (2011)
23. L. Deng, W. Lu, Z. Zhang, Z. Fu, H. Li, H. Chen, Y. Du, Y. Ma, W. Wang, Crystallization behavior and structure of CaO–MgO–Al_2O_3–SiO_2 glass ceramics prepared from Cr-bearing slag. Mater. Chem. Phys. **261**, 124249 (2021)
24. H. Wang, K. Cao, S. Jiao, G. Zhang, Enhanced performance of low-pressure sintered CaO–MgO–Al_2O_3–SiO_2–$CaCl_2$ glass-ceramic by using Cr_2O_3 as the nucleating agent. Ceram. Int. **50**, 14161–14170 (2024)
25. S. Son, K. Kim, Effect of TiO_2 content on crystallization behavior of CaO–Al_2O_3–SiO_2–ZnO glass-ceramic glaze. Ceram. Int. **49**, 13677–13686 (2023)
26. Z. Bao, S. Wang, L. Miao, Y. Xu, Z. Cheng, X. Wang, Preparation, properties and formation mechanism of transparent anorthite-based glass-ceramic glaze with high hardness. Ceram. Int., https://doi.org/10.1016/j.ceramint.2024.04.359
27. H. Hsiang, S. Yung, C. Wang, Crystallization, densification and dielectric properties of CaO–MgO–Al_2O_3–SiO_2 glass with ZrO_2 as nucleating agent. Mater. Res. Bull. **60**, 730–737 (2014)
28. S. Silakate, A. Wannagon, A. Nuntiya, Influence of ferric oxide on the crystallization of Li–Zn ferrite anorthite and hematite phases at low temperature ceramic glaze. J. Eur. Ceram. Soc. **35**, 2183–2188 (2015)
29. W. Zheng, H. Zhang, Q. Wang, J. Yuan, P. Tian, Effect of P_2O_5 on nucleation, crystallization and mechanical properties of Y_2O_3–Al_2O_3–SiO_2 glasses. Ceram. Int. **50**, 13467–13477 (2024)
30. B. Burzacchini, Use of the hot stage microscope to evaluate the characteristics and behaviour of frits and glazes at different heating rates. Proceeding of IV world congress on ceramic tile quality Qualicer, 701–709 (1996)
31. E.D. Zanotto, Viscous sintering with concurrent crystallization. Cryst. Glass. (2013). https://doi.org/10.1002/9781118559055.part3
32. K. Thieme, T. Zscheckel, C. Thieme, T. Höche, C. Rüssel, On the search for nucleation agents in BaO-SrO-ZnO-SiO_2 glasses: The influence of P_2O_5. J. Eur. Ceram. Soc. **38**, 2017–2026 (2018)
33. Z. Luo, H. Liang, C. Qin, T. Liu, A. Lu, Crystallization kinetics and phase formation of Li_2O-SiO_2-Si_3N_4 glass ceramics with P_2O_5 nucleating agent. J. Alloys Compd. **786**, 688–697 (2019)
34. Z.H. Bao, L.F. Miao, W.H. Jiang, J.M. Liu, J. Liang, T. Chen, Effect of B_2O_3 and P_2O_5 addition on the phase seperation and crystallization of Li_2O-MgO-Al_2O_3-SiO_2 glass-ceramics. Mater. Sci. Forum **848** (2016)
35. S.C. von Clausbruch, M. Schweiger, W. Höland, V. Rheinberger, The effect of P_2O_5 on the crystallization and microstructure of glass-ceramics in the SiO_2-Li_2O-K_2O-ZnO-P_2O_5 system. J. Non Cryst. Solids. **263**, 388–394 (2000)
36. W. Höland, E. Apel, C.V. Hoen, V. Rheinberger, Studies of crystal phase formation in high-strength lithium disilicate glass-ceramics. J. Non Cryst. Solids. **352**, 4041–4050 (2006)
37. H.R. Fernandes, D.U. Tulyaganov, J.M.F. Ferreira, The Role of P_2O_5, TiO_2 and ZrO_2 as nucleating agents on microstructure and crystallization behaviour of lithium disilicate-based glass. J. Mater. Sci. **48**(2), 765–773 (2013)
38. N. Ghaebi Panah, B. Eftekhari Yekta, V. Marghussian, E. Mohaghegh, Effects of TiO_2 and P_2O_5 on solarization and crystallization of photosensitive lithium silicate glass. J. Non Cryst. Solids. **430**, 25–30 (2015)
39. P. Glatz, M. Comte, L. Cormier, L. Montagne, B. Doumert, G.G. Moore, Different roles of phosphorus in the nucleation of lithium aluminosilicate glasses. J. Non Cryst. Solids. **493**, 48–56 (2018)
40. A. Gaddam, H.R. Fernandes, D.U. Tulyaganov, M.J. Ribeiro, J.M.F. Ferreira, The roles of P_2O_5 and SiO_2/Li_2O ratio on the network structure and crystallization kinetics of non-stoichiometric lithium disilicate based glasses. J. Non Cryst. Solids, 481 (2018)
41. M. Rampf, M. Fisch, G. Helsch et al., Quartz-containing glass-ceramics in the SiO_2–Li_2O–K_2O–MgO–CaO–Al_2O_3–P_2O_5 system. Int. J. Appl. Glass Sci. **10**(3), 330–338 (2019)

42. X. Zheng, G. Wen, L. Song, Effects of P_2O_5 and heat treatment on crystallization and microstructure in lithium disilicate glass ceramics. Acta Mater. **56**(3), 549–558 (2008)
43. N.-Z. Zhang, M. Zhang, H.-Y. Tang, L. Qin, C.-K. Cheng, P_2O_5 enhances the bioactivity of lithium silicate glass ceramics via promoting phase transformation and forming Li_3PO_4. Ceram. Int. **50**, 13308–13317 (2024)
44. H. Ahmadi, G. Khalaj, A. Najafi, S.M. Abbasi, M. Safari, Metakaolin-red mud/ carbon nanotubes geopolymer nanocomposite: Mechanical properties and structural studies. Mater. Res. Express. **9**(2), 025011 (2022)